Structural, electronic, and optical properties of hexagonal and triangular SiC NWs with different diameters*

Yan-Jing Li(李彦景)[1], Ya-Lin Li(李亚林)[2], Shu-Long Li(李树龙)[1], Pei Gong(龚裴)[1], and Xiao-Yong Fang(房晓勇)[1,†]

[1] *School of Science, Yanshan University, Qinhuangdao* 066004, *China*

[2] *Liren College, Yanshan University, Qinhuangdao* 066004, *China*

(Received 12 December 2016; revised manuscript received 3 February 2017; published online 10 March 2017)

Silicon carbide (SiC) is a wideband gap semiconductor with great application prospects, and the SiC nanomaterials have attracted more and more attention because of their unique photoelectric properties. According to the first-principles calculations, we investigate the effects of diameter on the electronic and optical properties of triangular SiC NWs (T-NWs) and hexagonal SiC NWs (H-NWs). The results show that the structure of H-NWs is more stable than T-NWs, and the conduction band bottom of H-NWs is more and more deviated from the valence band top, while the conduction band bottom of T-NWs is closer to the valence band top. What is more, H-NWs and T-NWs have anisotropic optical properties. The result may be helpful in developing the photoelectric materials.

Keywords: silicon carbon nanowires, stability, electronic properties, optical properties, first-principles theory

PACS: 73.61.Le, 81.07.Gf, 73.63.Nm, 78.67.Uh **DOI:** 10.1088/1674-1056/26/4/047309

1. Introduction

With the rapid development of nanoscience and nanotechnology, researchers have been intrigued by the different types of SiC nanostructures because of their excellent mechanical, thermal, electrical and optical properties,[1–5] which bode well for diverse applications in energy area,[6] biomedical engineering,[7] nanoelectronics, microelectronics,[8] microwave absorption, and electromagnetic shielding.[9] The SiC crystallizes in either a cubic or a hexagonal form, and exhibits interesting polytypism.[10,11] Lambrecht *et al.* figured up the band energies of 2H–SiC, 4H–SiC, 6H–SiC, and 3C–SiC bulk with the local-density approximation theory and compared with the experimental results[12] in 1994. Yao *et al.* firstly reported that though the 2H–SiC nanoscale structure produced by chemical reaction of silicon monoxide and methane many defects grew well along the [001] direction.[13] Bouziane *et al.* discovered that growing environment affected the magnetism of the dropped 3C–SiC.[14] Zhang *et al*. investigated the electronic structure and optical properties of single wall 2H–SiC nanotube.[15] Laref *et al*. found the saturated 3C–SiC NWs grown along the [001] direction were more stable when their diameters were bigger than those the ordinary 3C–SiC NWs.[16] The field emission properties of N-doped SiC nanowires were investigated by Zhao *et al*. in 2015.[17] Yang *et al*. reported for the first time electrochemical nitrite sensors based on SiC NWs with smooth surface and boron-doped cubic SiC NWs with fin-like structure.[18] However the reports about the optical and electrical properties of size dependent 2H–SiC with different diameters are relatively rare.

In fact, though more researches have been presented about SiC NWs[19] than other low-dimensional SiC nanostructures[20] theoretically and experimentally, the reports about 2H–SiC are quite limited. At low temperatures, 2H–SiC NWs are the most unstable in multiple structure of SiC, whereas the performance of 2H–SiC NWs is more stable if their diameters are less than 20 nm.[21] However, 3C–SiC NWs are more stable when their diameters are more than 20 nm. Consequently, the research on photo-electric properties of 2H–SiC NWs in small size is of great significance.

In our study, the lattice structures, electronic and the optical properties of the wurtzite SiC NWs along the [001] and [010] direction are investigated by using density functional theory calculations. We consider the band and the density of states of size dependent SiC NWs, besides, discuss reflectivity, absorption coefficients and loss coefficients and explain the relationship between the optical properties and the electronic structures finally.

2. Computational methods and models

2.1. Computational methods

The first-principle calculations are carried out by using the Cambridge Serial Total Energy Package (CASTEP) code with generalized gradient approximation (GGA) and Perdew–Burke–Ernzerhof function (PBE), which is used to

*Project supported by the National Natural Science Foundation of China (Grant No. 11574261) and the Natural Science Foundation of Hebei Province, China (Grant No. A2015203261).

†Corresponding author. E-mail: fang@ysu.edu.cn

© 2017 Chinese Physical Society and IOP Publishing Ltd

describe the exchange and correlation potentials. Under the one-dimensional periodic boundary condition, the plane wave functions are expanded for the multi-electronic system. Ultrasoft pseudopotentials (USP) have been employed to describe the interactions between the ion core and the valence electrons (C-2s2^2p^2 and Si-3s^{2}3p^2), reducing the number of the plane-wave bases. The plane-wave cutoff energy is set to be 300 eV and the k points are supposed to be $1\times1\times6$ under Monkhorst–Pack grid. The studied structures are adequately relaxed when the following convergence standards are satisfied: (i) the convergence standard of the individual-atom energy is 2.0×10^{-5}eV, (ii) the convergence standard of interaction between electrons is 0.05 eV/Å, (iii) the convergence standard for maximum shift of atom is 0.002 Å, and (iv) the convergence standard of crystal internal stress is 0.1 GPa.

2.2. Structural model

Build the three different diameters of the wurtzite SiC NW structures of the hexagonal and the triangular cross section. Add the vacuum layer in the radial direction, and take periodic boundary condition in the axial direction in order to ensure that the structures nearby do not interact with each other. The hexagonal SiC NWs are marked as H1 (48 atoms/cell), H2 (108 atoms/cell), H3 (192 atoms/cell), and the triangular SiC NWs are signed as T1 (44 atoms/cell), T2 (66 atoms/cell) and T3 (92 atoms/cell) respectively.

3. Results and discussion

3.1. Crystal structure and stability

The final relaxed structures are presented in Fig. 1. In each case, the structure is fully relaxed and the corresponding parameters, such as the crystal constant c, diameter D, bond length, total energy E_1 and cohesive energy E_2, are list in Table 1. The diameter is defined with respect to the position of carbon atoms at the sub-surface.

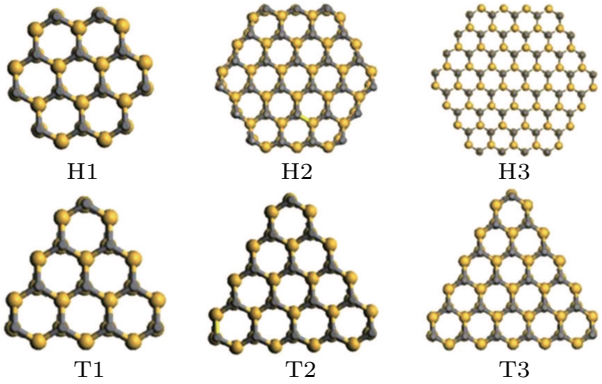


Fig. 1. (color online) Relaxed crystal structures of H1, H2, H3, T1, T2, and T3, where yellow (larger) and gray (smaller) ball represent silicon and carbon atoms respectively.

Table 1. Lattice structures and stability parameters of H-NWs and T-NWs.

SiC NWs structures	Diameter D/Å	Lattice constant c/Å	Si-C bond length/Å		Total energy E_1/eV	Cohesive energy E_2/eV
			Axial direction	Radial direction		
H1	9.461	5.164	1.869	1.901	–6289.037	–352.397
H2	15.31	5.094	1.993	1.902	–14154.35	–796.909
H3	21.45	5.087	1.993	1.907	–25181.05	–1434.49
T1	10.53	5.107	1.924	1.914	–5756.112	–314.192
T2	14.10	5.100	1.910	1.912	–8641.138	–478.258
T3	17.26	5.098	1.908	1.911	–12050.12	–671.561

As illustrated in Table 1, the lattice constant c is degenerated with the increase of the diameter in both cases, which accords well with the discussion below. The reductions of c in H-NWs are more evident than those in T-NWs.

The cohesive energy is utilized to weigh the structure stability: the smaller, the more stable. The cohesive energy is determined by

$$E_2 = E_1 - (E_{\mathrm{Si}} + E_{\mathrm{C}})N, \tag{1}$$

where N is the number of Si and C atomic couples, E_{Si} and E_{C} are the free energies of Si and C ($E_{\mathrm{Si}} = -101.52$ eV, $E_{\mathrm{C}} = -145.84$ eV), respectively. The cohesive energies of H-NWs and T-NWs are shown in Table 1. It can be seen that the cohesive energies of H-NWs and T-NWs decrease with the diameter increasing. Besides, the cohesive energies of H-NWs are smaller than those of T-NWs. This indicates that the structure of H-NWs is more stable than that of T-NWs under similar diameters.;oreover, with the diameter increasing the structures of the two morphologies of SiC NWs are more stable.

3.2. Electronic property

Figure 2 are the band structures of the H-NWs and T-NWs, where symbol ▲ denotes the position on the bottom of the conduction band (BCB), and symbol ▼ refers to the position on the top of the valence band (TVB), and the distances between the BCB and the TVB in the k-space are shown in Table 2. Figure 3 shows the band structures and densities of states of the H-NWs and T-NWs, and the data of the three peaks I, II, and III in the conduction band are shown in Table 2.

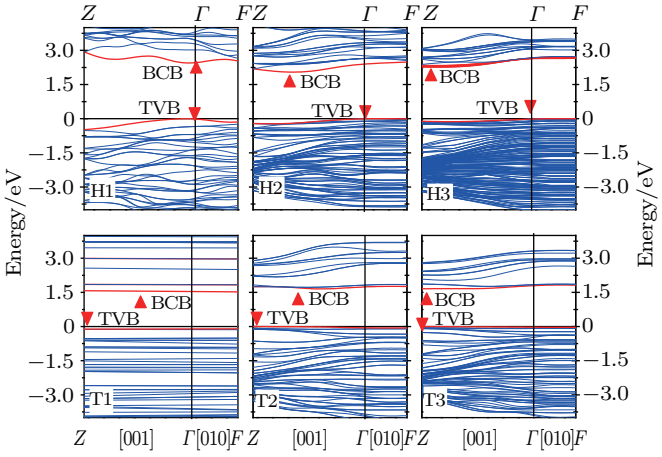


Fig. 2. (color online) Band structures of H-NWs and T-NWs.

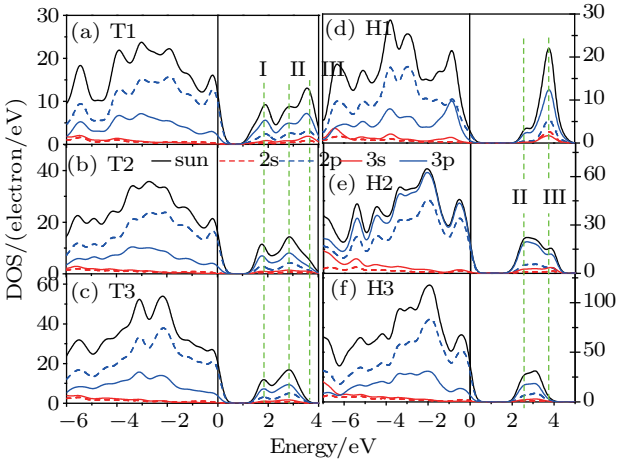


Fig. 3. (color online) Electronic density of states (DOS) for H-NWs and T-NWs.

Table 2. Energy band structures and electronic densities of states. Here Δk_{C-V} represents the interval between Γ point and Z point in Brillouin zone.

SiC NWs structures	Energy band structure		Conduction band width ΔE_C/eV	Density of states of the conduction band					
	Band gap E_g/eV	BCB position $\Delta k_{C-V}/(2\pi/c)$		Peak I		Peak II		Peak II	
				Position	Value	Position	Value	Position	Value
H1	2.44436	0	3.77	–	–	2.73	2.64	3.77	14.1
H2	2.05784	0.2909	3.68	–	–	2.70	22.3	3.81	15.6
H3	2.27102	0.4199	3.30	–	–	2.58	27.1	3.06	21.5
T1	1.37825	0.2064	4.24	1.88	6.48	2.83	5.77	3.52	9.06
T2	1.65308	0.2062	3.88	1.80	7.96	2.84	9.50	–	–
T3	1.65827	0.0874	3.48	1.83	8.29	2.80	11.1	–	–

From Figs. 2 and 3 and Table 2 some points can be extracted as follows.

(I) The top of the valence band (TVB) of H-NWs is in the center of the Brillouin zone (Γ point), and the top of valence band (TVB) of T-NWs is at the boundary of the Brillouin zone (Z point). No matter whether they are H-NWs or T-NWs, as the diameter increases, the bottom of conduction band (BCB) of them shifts along the [001] direction from the point Γ to the point Z. Therefore, with the diameter increasing, the BCB of H-NWs becomes far from the TVB, and the BCB of T-NWs is close to the TVB.

(II) Except H1-NWs (BVB and TCB are located at Γ point), the rest of SiC NWs are all indirect band gap semiconductors, moreover, the band gap E_g of T-NWs increases with the increase of the diameter, while there is no clear regulation for the gap of H-NWs.

(III) The TVB of the T-NWs is mainly determined by carbon 2p (C-2p), and the TVB of the H-NWs is determined by electronic of C-2p and Si-3p together, but as the diameter increases, the effect of 3p decreases. Whether the structure is triangular or hexagonal, the BCB is determined by the electronic of Si-3p.

(IV) DOS diagram shows that the tops of valence bands of the T-NWs and H-NWs cross the Fermi level, indicating that they are similar to that of boron-doped SiC and have P-type degenerate semiconductor properties.[22] But compared with the significant impurity level which is produced by doping, vacancy and other defects, owing to the fact that the unsaturated dangling bonds on the surface of SiC NWs will make the C-2p electrons lack, thereby causing the top of valence band energy density and the degeneracy to decrease,[23,24] the impurity level in Fig. 2 is not significant, indicating that the hole concentration in SiC NWs is very small.

(V) The density of states of the conduction band is composed of many peaks, which indicates that H-NWs and T-NWs both have quantum effect. (The energy band is composed of several discrete energy levels). As the diameter increases, density state of Si-3p is increased, however, as the width of conduction band narrows, the discrete energy level gradually becomes a quasi-continuous band, and the quantum effect is weakened.

3.3. Photoelectric properties

The optical dielectric constants of H-NWs and T-NWs with different diameters are shown in Fig. 4.

Figure 4 indicates some points below.

i) In addition to H1-NWs, the dielectric loss peak in the [001] direction is between 400 nm and 500 nm, and the dielectric loss peak in the [010] orientation is between 200 nm and 300 nm. Obviously, these dielectric constant spectrum con-

form to the Lorentz model, that is,[25]

$$\varepsilon = 1 + \frac{e^2 N}{m^* \varepsilon_0}\left[\frac{(\omega_0^2 - \omega^2)}{(\omega_0^2 - \omega^2)^2 + (\omega/\tau)^2} + \mathrm{i}\frac{\omega/\tau}{(\omega_0^2 - \omega^2)^2 + (\omega/\tau)^2}\right], \quad (2)$$

where τ represents the relaxation time and $\omega_0 = E_g/\hbar$. It can be seen that the optical dielectric constant of SiC NWs is mainly due to the electron displacement polarization between valence band and conduction band.

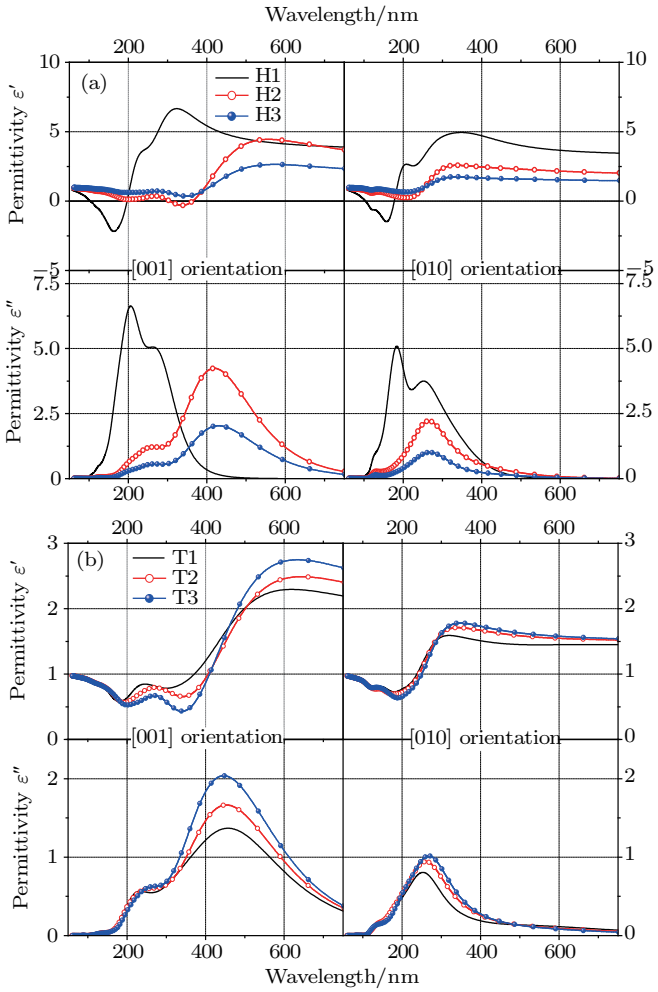


Fig. 4. (color online) Dielectric loss coefficients of H-NWs and T-NWs with different diameters.

ii) The optical dielectric constant of SiC NWs is obviously anisotropic. The result shows that the peak values of dielectric constant real and imaginary parts of the H-NWs and T-NWs in the [010] direction are smaller than those in the [001] direction, and the dielectric constant of the [010] direction is obviously blueshifted. This phenomenon from the band gap of [010] direction is more obvious than that from E_g (because of the conduction band bottom of SiC NWs in the [001] direction). Firstly, according to the electronic displacement polarization model

$$\alpha_e \approx 2Z\,|M_{cv}|^2/E_g, \quad (3)$$

the value of the dielectric constant in the [010] direction is less than in the [001] direction. Next, because the band gap in the [010] direction is larger than E_g, $\omega_0 > E_g/\hbar$, leads to the permittivity being shifted towards the high frequency in the [010] direction. In Eq. (3), M_{cv} denotes the dipole transition matrix elements between conduction band and valence band, and Zrepresents the number of valence electrons in the atom.

iii) The permittivity of H-NWs is larger than that of T-NWs under the similar diameter condition. While for H-NWs, the value decreases with increasing diameter, but the value of T-NWs is increased with diameter increasing. The reason is that with the increase of diameter, the conduction band bottom of H-NWs is far from the top of the valence band, and the conduction band bottom of T-NWs is close to the valence band top. As a result, the energy of H-NWs increases during interband transitions and the energy required for T-NWs decreases.[26]

Figures 5 and 6 show the spectral curves of reflectivity , absorption coefficient and loss coefficient for H-NWs and T-NWs with different diameters.

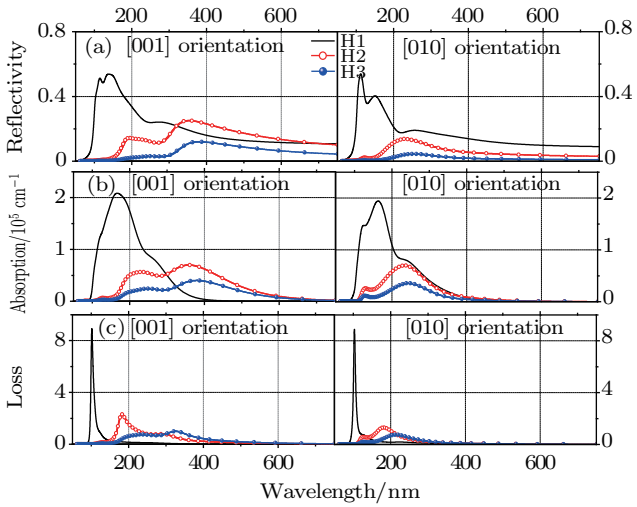


Fig. 5. (color online) Spectral curves of reflectivity, absorption coefficient, and loss coefficient of H-NWs with different diameters.

From Figs. 5 and 6, some points can be extracted below.

I) Like the dielectric constant spectrum, there are also two peaks in the spectra for reflectivity, absorption coefficient and loss coefficient in the [001] direction. Among them, the peak in the deep ultraviolet region comes from the interior valence electron transition, while the peak near the visible region comes from the electronic transition between valence band and conduction band.

II) H-NWs and T-NWs are anisotropic. The reflectivity, absorption coefficient and loss coefficient of H-NWs are all larger than those of T-NWs except H1-NWs in the [001] direction, while for H-NWs, the value decreases with increasing diameter, but the value increases with increasing diameter for T-NWs;

III) For H-NWs, except H1-NWs, the curve of absorption coefficient versus wavelength shows blue shift with diameter decreasing. For the first peak position of T-NWs, red shift occurs with the increase of diameter, the second peak position is blue-shifted with the increase of diameter, and the two peak positions are close to each other. Nevertheless, the relationships of reflectivity, absorption coefficients and loss coefficients with the wavelength are similar.

IV) In general, the energy required for the indirect electron transition is less than for the direct transition, that is, the corresponding wavelength should be greater than the wavelength required for the direct transition, moreover, the absorption waveform near the absorption edge of the indirect band gap semiconductor is smoother.[26] It can be concluded that H1-NWs of a direct band gap and the rest are of indirect band gap, which is consistent with the analysis results in Fig. 2.

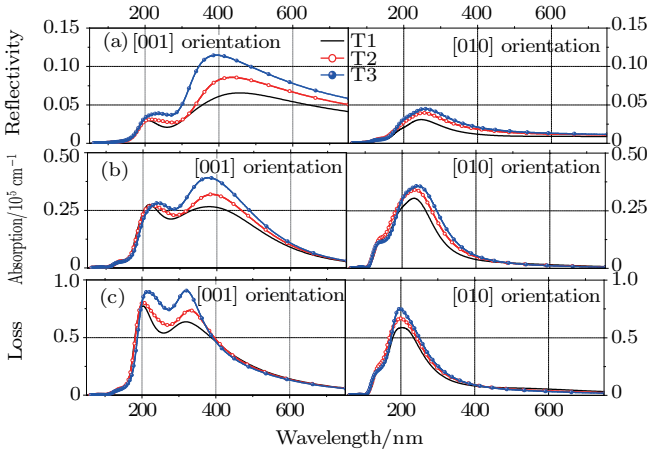


Fig. 6. (color online) Spectral curves of reflectivity, absorption coefficient, and loss coefficient of T-NWs with different diameters

4. Conclusions

In this work, we study the effects of diameter on the stability, electronic and optical properties of H-NWs and T-NWs by using first-principle calculations. The electronics of NWs is analysed, showing that except H1-NWs, all the remaining SiC NWs are indirect band gap semiconductors, whereas the optical properties show that H-NWs and T-NWs are obviously anisotropic and that the structure of H-NWs is more stable than that of T-NWs. The values of absorption coefficient, reflectivity and loss coefficient in the axial direction are larger than those in the radial direction, for which the reason is that the radial direction of NWs is restricted. The results have a definite influence on the development of photoelectric materials.

References

[1] Cheng G, Chang T H, Qin Q, Huang H and Zhu Y 2014 *Nano Lett.* **14** 754
[2] Phan H P, Dinh T, Kozeki T, Nguyen T K, Qamar A, Namazu T, Nguyen NT and Dao D V 2016 *IEEE Electron Dev. Lett.* **37** 1029
[3] Gali A 2006 *Phys. Rev. B* **73** 245415
[4] Xiong S, Latour B, Ni Y, Volz S and Chalopin Y 2015 *Phys. Rev. B* **91** 224307
[5] Konstantinos T, Thibaut B, Ni Y X, Samy M, Xanthippi Z, Yann C, Patrice C and Sebastian V 2013 *Phys. Rev. B* **87** 125410
[6] Mukherjee S and Ray A K 2008 *J. Comput. Theor. Nanosci.* **5** 1210
[7] Medintz I L, Uyeda H T, Goldman E R and Mattoussi H 2005 *Nat. Mater.* **4** 435
[8] Zhu J, Wu Y D, Chen H T, Xiong X and Chen X B 2012 *Micro Nano Lett.* **7** 974
[9] Duan W, Yin X, Cao F, Jia Y, Xie Y, Greil P and Travitzky N 2015 *Mater. Lett.* **159** 257
[10] Wyckoff W G 1963 *Crystal Structures* (John Wiley And Sons) p. 1
[11] Ivanov P A and Chelnokov V E 1992 *Semiconductor. Sci. Technol.* **7** 863
[12] Lambrecht W R L, Segall B, Yoganathan M, Suttrop W, Devaty R P, Choyke W J, Edmond J A, Powell J A and Alouani M 1994 *Phys. Rev. B* **50** 722
[13] Yao Y, Lee S T and Li F H 2003 *Chem. Phys. Lett.* **381** 628
[14] Bouziane K, Mamor M, Elzain M, Djemia and Chérif S M 2008 *Phys. Rev. B* **78** 195305
[15] Zhang W H, Zhang F C, Zhang Z Y, Lu S Y and Yang Y N 2010 *Sci. China- Phys. Mech. Astron.* **53** 1582
[16] Laref A, Alshammari N, Laref S and Luo S J 2014 *Dalton Trans.* **43** 5505
[17] Zhao J, Meng A and Zhang M 2015 *Phys. Chem. Chem. Phys.* **17** 28658
[18] Yang T, Zhang L and Hou X 2016 *Sci. Rep.* **6** 24872
[19] Fan J Y and Chu P K 2014 *Engineering Materials and Processes* (Switzerland Springer) p. 258
[20] Li H, Wu J and Wang Z M 2013 *Silicon-based Nanomaterials*, Springer Series in Materials Science 187 pp. 139–157
[21] Ito Tomonori, Kosuke Sano, Toru Akiyama, *et al.* 2006 *Thin Solid Films* **508** 243
[22] Feng G Y, Fang X Y, Wang J J, Zhou Y, Lu R, Yuan J and Cao M S 2010 *Physica B* **405** 2625
[23] Rosso E F and Baierle R J 2013 *Chem. Phys. Lett.* **568–569** 140
[24] Yu X X, Zhou Y, Liu J, Jin H B, Fang X Y and Cao M 2015 *Chin. Phys. B* **24** 127307
[25] Zheng H M, Fang X Y, Cai L X, Yin A C, Jin H B, Yu X X and Cao M S 2014 *Chin. Phys. B* **23** 126102
[26] Wang K, Fang X Y, Li Y Q, Yin A C, Jin H B, Yuan J and Cao M S 2012 *J. Appl. Phys.* **112** 033508